

## Study $\omega$ and $\phi$ photoproduction in the nucleon isotopic channels

Q. Zhao

*Department of Physics, University of Surrey, Guildford, GU2 7XH, UK*  
*E-mail: qiang.zhao@surrey.ac.uk*

We present results for the photoproduction of  $\omega$  and  $\phi$  meson in the nucleon isotopic channels. A recently developed quark model with an effective Lagrangian is employed to account for the non-diffractive  $s$ - and  $u$ -channel processes; the diffractive feature arising from the *natural* parity exchange is accounted for by the  $t$ -channel pomeron exchange, while the *unnatural* parity exchange is accounted for by the  $t$ -channel pion exchange. In the  $\omega$  production, the isotopic effects could provide more information concerning the search of “missing resonances”, while in the  $\phi$  production, the isotopic effects could highlight non-diffractive resonance excitation mechanisms at large angles.

### 1 Introduction

The availabilities of high intensity electron and photon beams at JLab (CLAS), ELSA (SAPHIR), MAMI, ESRF (GRAAL), and SPring-8 give accesses to excite nucleons with the clean electromagnetic probes, thus revive the interest in the search of “missing resonances”<sup>1</sup> in meson photo- and electroproduction. Vector meson photoproduction near threshold attracts attentions<sup>2,3,4,5,6</sup> since those “missing resonances” could have stronger couplings to this channel such that their existing signals might be derived.

Taking into account large degrees of freedom in the resonance excitations, experimental efforts for such a purpose is by no means trivial. Historically, experimental data for photoproduction of vector meson in isotopic channels are very sparse. In contrast with the reaction  $\gamma + p \rightarrow \omega(\rho^0) + p$ , there are only few dots available for  $\gamma + n \rightarrow \rho^- + p$  and  $\gamma + p \rightarrow \rho^+ + n$ , while experiment on  $\gamma + n \rightarrow \omega(\phi) + n$  is not available. The main feature in the latter reactions is that the electric transition vanishes in the nucleon pole terms. Nevertheless, due to the change of the isospin degrees of freedom, interferences between different resonances and processes will change significantly. Nevertheless, in the neutron target reaction, resonances of quark model representation [70, 48] are no longer suppressed by the Moorhouse selection rule<sup>7</sup>, thus will add more ingredients into the reaction. Briefly, apart from various polarization observables which could provide rich information about the reaction mechanism, coherent study of isotopic reactions could also highlight signals which cannot be seen easily in a single channel.

Our motivation of studying the isotopic production of the  $\phi$  meson is rather different from the  $\omega$ . Our attention here is paid to the effects from the non-

diffractive  $s$ - and  $u$ -channel  $\phi$  production in polarization observables. The study of isotopic reaction provides us with insights into the non-diffractive processes at large angles (large momentum transfer with  $W \approx 2 \sim 4$  GeV). Since the  $\phi$  meson has higher threshold ( $E_\gamma \approx 1.57$  GeV), where a large number of resonances can be excited, the non-diffractive resonance effects could exhibit more collectively rather than exclusively from individual resonances. Another relevant interest in  $\phi$  production is to detect strangeness component in nucleons, which could be another important non-diffractive source in the reaction<sup>8,9,10</sup>. Although our study does not take into account such a mechanism, we shall see that our results provide some supplementary information for such an effort.

In this proceeding, a quark model approach to vector meson photoproduction<sup>2,3,11,12</sup> is applied to the photoproduction of  $\omega$  and  $\phi$  meson off the proton and neutron. Our purpose is to provide a framework on which a systematic study of resonance excitations becomes possible.

## 2 The model

Our model consists of three processes: (i) vector meson production through an effective Lagrangian; (ii)  $t$ -channel pomeron exchange ( $\mathcal{P}$ ) for  $\omega$ ,  $\rho^0$  and  $\phi$  production<sup>13</sup>; (iii)  $t$ -channel light meson exchange. Namely, in the  $\omega$  and  $\phi$  meson photoproduction, the  $\pi^0$  exchange ( $\pi$ ) is taken into account.<sup>a</sup>

The effective Lagrangian for the  $V$ - $qq$  coupling is:

$$L_{eff} = \bar{\psi}(a\gamma_\mu + \frac{ib\sigma_{\mu\nu}q^\nu}{2m_q})V^\mu\psi, \quad (1)$$

where  $\psi$  ( $\bar{\psi}$ ) denotes the light quark (anti-quark) field in a baryon system;  $V^\mu$  represents vector meson field ( $\omega$ ,  $\rho$ ,  $K^*$  and  $\phi$ ). In this model, the 3-quark baryon system is described by the NRCQM in the  $SU(6) \otimes O(3)$  symmetry limit, while the vector meson is treated as an elementary point-like particle which couples to the constituent quark through the effective interaction. Parameter  $a$  and  $b$  denote the coupling strengths and are determined by experimental data.

The tree level transitions from the effective Lagrangian can be labelled by the Mandelstam variable,  $s$ ,  $u$ , and  $t$ :

$$M_{fi} = M_{fi}^s + M_{fi}^u + M_{fi}^t. \quad (2)$$

Given the electromagnetic coupling  $H_e = -\bar{\psi}\gamma_\mu e_q A^\mu\psi$ , and the effective strong coupling  $H_m = -\bar{\psi}(a\gamma_\mu + \frac{ib\sigma_{\mu\nu}q^\nu}{2m_q})V^\mu\psi$ , the  $s$ - and  $u$ -channel with resonance

<sup>a</sup>In the  $\rho^0$  production, the  $\sigma$  meson exchange is included.

excitations can be expressed as,

$$\begin{aligned}
M_{fi}^{s+u} &= \sum_j \langle N_f | H_m | N_j \rangle \langle N_j | \frac{1}{E_i + \omega_\gamma - E_j} H_e | N_i \rangle \\
&+ \sum_j \langle N_f | H_e \frac{1}{E_i - \omega_m - E_j} | N_j \rangle \langle N_j | H_m | N_i \rangle, \quad (3)
\end{aligned}$$

where  $\omega_\gamma$  and  $\omega_m$  represent the photon and meson energy, respectively. In this expression, all the intermediate states  $|N_j\rangle$  are included. A simple transformation for the electromagnetic interaction leads to,

$$\begin{aligned}
M_{fi}^{s+u} &= i \langle N_f | [g_e, H_m] | N_i \rangle \\
&+ i\omega_\gamma \sum_j \langle N_f | H_m | N_j \rangle \langle N_j | \frac{1}{E_i + \omega_\gamma - E_j} h_e | N_i \rangle \\
&+ i\omega_\gamma \sum_j \langle N_f | h_e \frac{1}{E_i - \omega_m - E_j} | N_j \rangle \langle N_j | H_m | N_i \rangle, \quad (4)
\end{aligned}$$

with  $h_e = \sum_l e_l \mathbf{r}_l \cdot \boldsymbol{\epsilon}_\gamma (1 - \boldsymbol{\alpha} \cdot \hat{\mathbf{k}}) e^{i\mathbf{k} \cdot \mathbf{r}_l}$ , and  $g_e = \sum_l e_l \mathbf{r}_l \cdot \boldsymbol{\epsilon}_\gamma e^{i\mathbf{k} \cdot \mathbf{r}_l}$ , where  $\hat{\mathbf{k}} \equiv \mathbf{k}/\omega_\gamma$  is the unit vector along the photon three-momentum  $\mathbf{k}$ . We identify the term  $i \langle N_f | [g_e, H_m] | N_i \rangle$  as a seagull term  $M_{fi}^{sg}$ , and re-define the second and third term as the  $s$ - and  $u$ -channel, respectively. The tree level diagrams are illustrated in Fig. 1, where a bracket on the seagull term gives a caution about its origin.

In the NRCQM, those low-lying states ( $n \leq 2$ ) have been successfully related to the resonances which can be taken into account explicitly in the formula. For those higher excited states, they can be treated degenerate in the main quantum number  $n$  in the harmonic oscillator basis. Detailed description of this approach can be found in Ref. <sup>2,11,3</sup>. The  $\omega$  and  $\phi$  production are significantly simplified because of isospin conservation. Namely, only isospin 1/2 intermediate resonances will contribute in the reaction. Another advantage for these two reactions is that both particles are charge-neutral. This feature leads to the vanishing of the  $t$ -channel vector meson exchange and the seagull term. In the end, only the  $s$ - and  $u$ -channel (S+U) from Eq. 4 will be the contribution source from the effective Lagrangian. In addition, the Moorhouse selection rule<sup>7</sup> further simplifies the calculations for the proton target reaction. Due to this selection rule, resonances belonging to representation  $[\mathbf{70}, \mathbf{48}]$  would vanish in the  $\gamma p \rightarrow N^*$  transitions.

Apart from the S+U from the effective Lagrangian, our model includes the pomeron exchange ( $\mathcal{P}$ ) to account for the diffractive phenomenon in vector

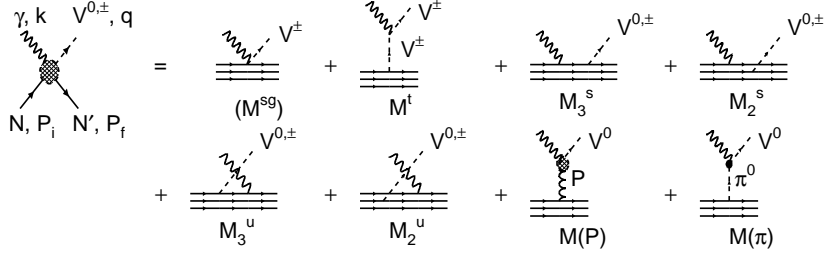


Figure 1: Tree level transition diagrams for the reaction.

meson photoproduction. In this model<sup>13</sup>, the pomeron mediates the long range interaction between two confined quarks, and behaves rather like a  $C = +1$  isoscalar photon. We summarize the vertices as follows:

(i) pomeron-nucleon coupling:

$$F_\mu(t) = 3\beta_0\gamma_\mu f(t), \quad f(t) = \frac{(4M_N^2 - 2.8t)}{(4M_N^2 - t)(1 - t/0.7)^2}, \quad (5)$$

where  $\beta_0 = 1.27 \text{ GeV}^{-1}$  is the coupling of the pomeron to one light constituent quark;  $f(t)$  is the isoscalar nucleon electromagnetic form factor with four-momentum transfer  $t$ ; the factor 3 comes from the “quark-counting rule”.

(ii) Quark- $\phi$ -meson coupling:

$$V_\nu(p - \frac{1}{2}q, p + \frac{1}{2}q) = f_V M_\phi \gamma_\nu, \quad (6)$$

where  $f_V$  is the radiative decay constant of the vector meson, and determined by  $\Gamma_{V \rightarrow e^+e^-} = 8\pi\alpha_e^2 e_Q^2 f_V^2 / 3M_V$ . A form factor  $\mu_0^2 / (\mu_0^2 + p^2)$  is adopted for the pomeron-off-shell-quark vertex, where  $\mu_0 = 1.2 \text{ GeV}$  is the cut-off energy, and  $p$  is the four-momentum of the quark. The pomeron trajectory is  $\alpha(t) = 1 + \epsilon + \alpha' t$ , with  $\alpha' = 0.25 \text{ GeV}^{-2}$ .

The  $\pi^0$  exchange is introduced with the following Lagrangians for the  $\pi NN$  and  $\phi\pi\gamma$  coupling:

$$L_{\pi NN} = -ig_{\pi NN} \bar{\psi} \gamma_5 (\boldsymbol{\tau} \cdot \boldsymbol{\pi}) \psi. \quad (7)$$

and

$$L_{V\pi^0\gamma} = e_N \frac{g_{V\pi\gamma}}{M_V} \epsilon_{\alpha\beta\gamma\delta} \partial^\alpha A^\beta \partial^\gamma V^\delta \pi^0 . \quad (8)$$

where the commonly used couplings,  $g_{\pi NN}^2/4\pi = 14$ ,  $g_{\omega\pi\gamma}^2 = 3.315$  and  $g_{\phi\pi\gamma}^2 = 0.143$ , are adopted.

An exponential factor  $e^{-(\mathbf{q}-\mathbf{k})^2/6\alpha_\pi^2}$  from the nucleon wavefunctions plays a role as a form factor for the  $\pi NN$  and  $\phi\pi\gamma$  vertices, where  $\alpha_\pi = 300$  MeV is adopted. This factor comes out naturally in the harmonic oscillator basis where the nucleon is treated as a 3-quark system.

### 3 Results and discussions

Application of this approach to the  $\omega$  meson photoproduction shows a great promise. A coherent study of the  $\rho$  meson photoproduction<sup>2</sup> also highlights the approximately satisfied isospin symmetry between the  $\omega$  and  $\rho$  meson.

In  $\gamma p \rightarrow \omega p$ , the old measurements<sup>14</sup> of the parity asymmetries at  $E_\gamma = 2.8, 4.7$  and  $9.3$  GeV provides very strong constraints on the *natural* ( $\mathcal{P}$ ) and *unnatural*-parity exchange ( $\pi$ ). It was shown that at  $E_\gamma = 2.8$  GeV, the parity asymmetry has a negative value which suggests the still dominant contribution from the pion exchange. At  $4.7$  GeV, the *natural*-parity starts to dominate over the cross section, and at  $9.3$  GeV, the parity asymmetry is completely dominated by the pomeron exchanges. Such an energy evolution of the parity asymmetry above the resonance region constrains the ‘‘background’’ terms, which then can be extrapolated down to the resonance region. In Ref.<sup>3,15</sup>, we show that such a scheme is consistent with the experimental data for the parity asymmetries<sup>14</sup>, and indeed leads to a reasonable estimation of these ‘‘background’’ terms.

#### 3.1 $\omega$ meson photoproduction

Parameters at resonance region for the  $\omega$  photoproduction are constrained approximately by the SAPHIR data<sup>16</sup>. It shows that  $a = -2.72$  and  $b' \equiv b - a = -3.42$  give an overall fit of available data.

In Fig. 2, differential cross sections for the isotopic channels are presented at four energy bins,  $E_\gamma = 1.225, 1.450, 1.675$  and  $1.915$  GeV, and compared with the SAPHIR data<sup>16</sup>. It shows that near threshold the  $\pi^0$  exchange ( $\pi$ ) dominates over the other two processes at small angles, while  $\mathcal{P}$  will compete with  $\pi$  with the increasing energies. The exclusive  $\mathcal{P}$  and  $\pi$  in the proton and neutron reaction are changed slightly due to the small difference between the proton and neutron mass. The S+U contributions generally dominate at large

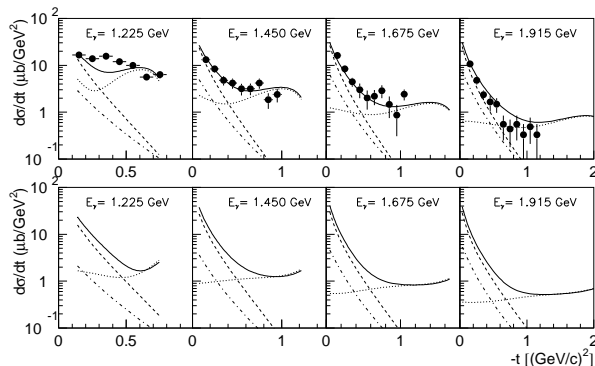


Figure 2: Differential cross section for  $\gamma p \rightarrow \omega p$  (upper column) and  $\gamma n \rightarrow \phi n$  (lower column). The dashed, dot-dashed, and dotted curves denote exclusive results for process, S+U,  $\mathcal{P}$  and  $\pi$ , respectively; the solid curves represent full model calculation. Data are from Ref. 16.

angles. Compare these two isotopic reactions, we see that the main impact of the change of the isospin space comes from S+U.

Interesting interfering effects among these processes could be seen in polarization observables. In Fig. 3, we present predictions for  $\Sigma \equiv (2\rho_{11}^1 + \rho_{00}^1)/(2\rho_{11}^0 + \rho_{00}^0)$ , which has been measured by GRAAL<sup>17</sup>. Here,  $\rho^1$  and  $\rho^0$  are density matrix elements in the helicity space<sup>18</sup>. One important feature of  $\Sigma$  is that large asymmetries (deviation from 0) cannot be produced by the exclusive  $\mathcal{P}$ ,  $\pi$  or  $\mathcal{P} + \pi$ . As shown by the solid curves, large asymmetries are produced by the interferences between the  $\mathcal{P} + \pi$  and S+U processes. Interest arises from the comparison of the isotopic reactions. It shows that the S+U produces flattened positive asymmetries in  $\gamma n \rightarrow \omega n$  near threshold. Specifically, we show the effects of  $P_{13}(1720)$  in the  $\Sigma$ , which suggest that isotopic reactions could have outlined more information.

Another interesting observable with polarized photon beam is,  $\Sigma_A \equiv (\rho_{11}^1 + \rho_{1-1}^1)/(\rho_{11}^0 + \rho_{1-1}^0)$ . As found in Ref. 3, this observable is more sensitive to small contributions from individual resonances. Due to lack of space, we shall only show the calculation of  $\Sigma_A$  for the  $\phi$  production in the next Subsection.

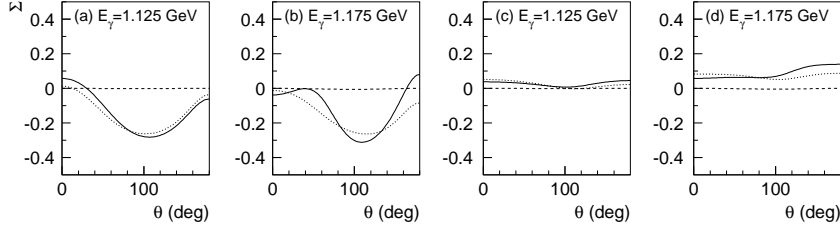


Figure 3: Polarized beam symmetry for the proton [(a)-(b)] and neutron reactions [(c)-(d)] in  $\omega$  production. The solid, dashed, and dotted curves denote the full model calculation,  $\mathcal{P} + \pi$ , the full model excluding the  $P_{13}(1720)$ .

### 3.2 $\phi$ meson photoproduction

In the  $\phi$  meson production, the parameter  $a = 0.241 \pm 0.105$  and  $b' \equiv b - a = 0.458 \pm 0.091$  for the effective  $\phi$ - $qq$  coupling are determined by the fit of old data from Ref. <sup>19</sup> at  $E_\gamma = 2.0$  GeV and the recent data from CLAS <sup>20</sup> at 3.6 GeV. These values are much smaller than parameters derived for the  $\omega$  and  $\rho$  production. Qualitatively, the  $\phi$ - $qq$  couplings could be suppressed by the OZI rule. Meanwhile, in the SU(3) symmetry limit,  $a_\phi/a_\omega = g_{\phi NN}/g_{\omega NN}$  can be derived, which is consistent with the ratio for an ideal  $\omega$ - $\phi$  mixing <sup>21</sup>,  $g_{\phi NN}/g_{\omega NN} = -\tan 3.7^\circ$ .

Using the same parameters derived in  $\gamma p \rightarrow \phi p$ , the cross sections for both  $\gamma p \rightarrow \phi p$  and  $\gamma n \rightarrow \phi n$  are calculated at  $E_\gamma = 2.0$  GeV (Fig. 4). Significant cross section difference occurs at large angles, where  $d\sigma/d\Omega$  for  $\gamma n \rightarrow \phi n$  is much smaller than for  $\gamma p \rightarrow \phi p$ . A common feature arising from these two reactions is a relatively stronger backward peak from the “background”  $u$ -channel nucleon pole term. Similar feature is also found by Laget <sup>22</sup>.

In Fig. 5, the isotopic effects of these two reactions are shown for the polarized beam asymmetry  $\Sigma_A \equiv (\rho_{11}^1 + \rho_{1-1}^1)/(\rho_{11}^0 + \rho_{1-1}^0) = (\sigma_{\parallel} - \sigma_{\perp})/(\sigma_{\parallel} + \sigma_{\perp})$  at  $E_\gamma = 2.0$  GeV, where  $\sigma_{\parallel}$  and  $\sigma_{\perp}$  denote the cross sections for  $\phi \rightarrow K^+K^-$  when the decay plane is parallel or perpendicular to the photon polarization vector.

The dashed curves represent results for  $\mathcal{P} + \pi$ , which deviate from +1 (for pure *natural*-parity exchange) due to the presence of the *unnatural* parity pion exchange. With the S+U, the full model calculation suggests that the large angle asymmetry is strongly influenced by the S+U processes, while the forward angles are not sensitive to them. Interferences between the  $\mathcal{P}$  and

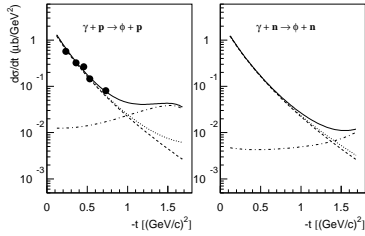


Figure 4: Differential cross section for  $\phi$  production at  $E_\gamma = 2.0$  GeV. The dot-dashed, dashed, and solid curves denote the S+U,  $\mathcal{P} + \pi$ , and full model calculations, respectively, while the dotted curve represents full model calculation excluding the  $u$ -channel contribution. Data come from Ref. <sup>19</sup>.

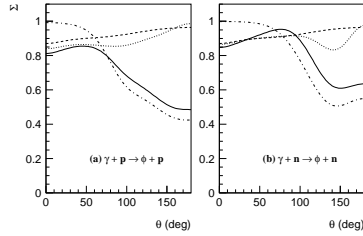


Figure 5: Polarized beam symmetry  $\Sigma_A$  for the proton and neutron reactions at  $E_\gamma = 2.0$  GeV. Notations are the same as Fig. 4.

S+U can be seen by excluding the  $\pi$  (see the dot-dashed curves). It shows that asymmetries produced by the S+U at forward angles are negligible. Since the pion exchange becomes very small at large angles, we conclude that the large angle asymmetry is determined by the S+U and reflects the isotopic effects. The role played by the  $s$ -channel resonances in the two reactions are presented by excluding the  $u$ -channel contributions. As shown by the dotted curves, the interferences from the  $s$ -channel resonances are much weaker than that from the  $u$ -channel, although they are still an important non-diffractive source at large angles.

This feature, which might make it difficult to filter out signals for individual  $s$ -channel resonances in the  $\phi$  photoproductions might suggest that the forward angle could be an ideal region for the study of other non-diffractive sources. <sup>b</sup>

It should be noted that no isotopic effects can be seen in  $\Sigma$  and  $\Sigma_A$  if only  $\mathcal{P} + \pi$  contribute to the cross section. This is because the transition amplitude of  $\mathcal{P}$  is purely imaginary, while that of pion exchange is purely real. In  $\Sigma$  and  $\Sigma_A$ , the sign arising from the  $g_{\pi NN}$  will disappear, which is why the dashed curves in Fig. 5 are (almost) the same. It is worth noting that our results for the  $\Sigma_A$  are quite similar to findings of Ref. <sup>23</sup> at small angles, but very different at large angles. In Ref. <sup>23</sup> only the nucleon pole terms for the  $s$ - and  $u$ -channel

<sup>b</sup> For example, it was suggested by Ref. <sup>8,9</sup>, the strangeness component in nucleons could produce large asymmetries in beam-target double polarization observable at forward angles, while we find that S+U process only make sense at large angles. <sup>11,12</sup>



processes were included.

#### 4 Conclusions and perspectives

We show that the effective Lagrangian approach in the quark model basis provides an ideal framework for the study of resonance excitations in vector meson photoproduction. The great advantage is that only a limited number of parameters will be introduced. Meanwhile, it permits a systematic and coherent study of different isospin channels, which could be helpful in highlighting model-independent features in the reaction mechanisms. In the  $SU(6)\otimes O(3)$  framework, photoproduction of isospin 1 ( $\rho^{0,\pm 1}$ ) and isospin 1/2 ( $K^{*\pm}$ ,  $K^{*0}$  and  $\bar{K}^{*0}$ ) can be also studied<sup>2,24</sup>.

Concerning the search of signals for  $s\bar{s}$  component in the nucleon, the forward angle kinematics might be selective if the findings of Refs.<sup>9,10</sup> are taken into account, since effects from the S+U are negligible. Certainly, since a possible strangeness content has not been explicitly included in this model, the effective  $\phi$ - $qq$  coupling cannot distinguish between an OZI evading  $\phi NN$  coupling and a strangeness component in the nucleon. In future study, a more complex approach including the possible strangeness component in the nucleon should be explored.

Concerning the efforts of searching for “missing resonances” (in  $\omega$  photoproduction)<sup>25</sup> and probing strangeness components (in  $\phi$ )<sup>26,27</sup>, it shows that the isotopic channels might be useful for disentangling various processes involved in the reaction mechanism. Experiments using the neutron target could provide more evidence to pin down model-independent aspects for any modelling<sup>28</sup>.

#### Acknowledgments

I thank J.-P. Didelez, M. Guidal, B. Saghai, and J.S. Al-Khalili for collaborations on part of the work. Fruitful discussions with E. Hourany concerning the GRAAL experiment, T. Nakano concerning the SPring-8, and P.L. Cole and D.J. Tedeschi concerning the CLAS experiments, are acknowledged.

1. N. Isgur and G. Karl, *Phys. Lett. B* **72**, 109 (1977); *Phys. Rev. D* **23**, 817 (1981); R. Koniuk and N. Isgur, *Phys. Rev. D* **21**, 1868 (1980); S. capstick and W. Roberts, *Phys. Rev. D* **49**, 4570 (1994).
2. Q. Zhao, Z.-P. Li and C. Bennhold, *Phys. Lett. B* **436**, 42 (1998); *Phys. Rev. C* **58**, 2393 (1998).
3. Q. Zhao, *Phys. Rev. C* **63**, 025203 (2001).
4. Y. Oh, A.I. Titov and T.-S.H. Lee, *Phys. Rev. C* **63**, 025201 (2001).

5. Y. Oh, proceeding of this conference.
6. A.I. Titov, proceeding of this conference.
7. R.G. Moorhouse, *Phys. Rev. Lett.* **16**, 772 (1966).
8. E.M. Henley, G. Krein, and A.G. Williams, *Phys. Lett. B* **281**, 178 (1992).
9. A.I. Titov, Y. Oh, and S.N. Yang, *Phys. Rev. Lett.* **79**, 1643 (1997).
10. A.I. Titov, Y. Oh, S.N. Yang, and T. Morii, *Phys. Rev. C* **58**, 2429 (1998).
11. Q. Zhao, J.-P. Didelez, M. Guidal, and B. Saghai, *Nucl. Phys. A* **660**, 323 (1999).
12. Q. Zhao, B. Saghai and J.S. Al-Khalili, *Phys. Lett. B* **509**, 231 (2001).
13. A. Donnachie and P.V. Landshoff, *Phys. Lett. B* **185**, 403 (1987); *Nucl. Phys. B* **311**, 509 (1989).
14. J. Ballam *et al.*, *Phys. Rev. D* **7**, 3150 (1973).
15. Q. Zhao, proceeding of NSTAR2001 (Mainz), p237, World Scientific, 2001.
16. F.J. Klein, Ph.D. thesis, Univ. of Bonn, Bonn-IR-96-008 (1996);  $\pi$ N Newslett. 14, 141 (1998).
17. J. Ajaka *et al.*, Proceeding of the 14th International Spin Physics Symposium, Osaka, Japan, October 16-21, 2000.
18. K. Schilling, P. Seyboth, and G. Wolf, *Nucl. Phys. B* **15**, 397 (1970).
19. H.J. Besch *et al.*, *Nucl. Phys. B* **70**, 257 (1974).
20. CLAS Collaboration, E. Anciant *et al.*, *Phys. Rev. Lett.* **85**, 4682 (2000).
21. Particle Data Group, D.E. Groom *et al.*, *Euro. Phys. J. C* **15**, 1 (2000).
22. J.-M. Laget, *Phys. Lett. B* **489**, 313 (2000).
23. A.I. Titov, T.-S.H. Lee, and H. Toki, *Phys. Rev. C* **59**, R2993 (1999).
24. Q. Zhao, J.S. Al-Khalili and C. Bennhold, *Phys. Rev. C* **64**, 052201(R) (2001).
25. P.L. Cole, proceeding of this conference.
26. T. Nakano, proceeding of this conference.
27. D.J. Tedeschi, proceeding of this conference.
28. J.-P. Didelez, proceeding of this conference, and private communication.